available at www.sciencedirect.com

www.elsevier.com/locate/matchar

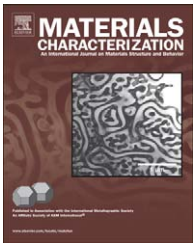

Effects of ultrasonic processing on phase transition of flame-synthesized anatase TiO_2 nanoparticles

Gyo Woo Lee[a,*], *Jeong Hoon Byeon*[b]

[a]*Division of Mechanical Design Engineering, Chonbuk National University, Jeonju 561-756, Republic of Korea*
[b]*Samsung Electronics Co. Ltd., Suwon 443-742, Republic of Korea*

ARTICLE DATA

Article history:
Received 27 October 2008
Received in revised form 28 July 2009
Accepted 5 August 2009

Keywords:
Phase transformation
TiO_2 nanoparticles
Ultrasonic processing
SEM
BET
XRD

ABSTRACT

The effect of ultrasonic processing on the phase transformation of flame-synthesized anatase TiO_2 nanoparticles heated to the rutile phase was investigated. TiO_2 nanoparticles of various sizes were prepared using a coflow hydrogen diffusion flame and an ultrasonic processor. Smaller nanoparticles having a similar portion of anatase phase using the ultrasonic processor were produced. On the basis of scanning electron microscopy images and specific surface areas, we observed that smaller nanoparticles tended to be sintered more easily than larger nanoparticles. From X-ray diffraction analysis, we demonstrated that when heated, TiO_2 nanoparticles synthesized using the ultrasonic processor at 60% of its maximum amplitude were transformed from the anatase phase to the rutile phase more easily than those formed without or with the ultrasonic processor operated at 20% of its maximum amplitude.

1. Introduction

TiO_2 nanoparticles are a well-known photocatalyst. Photocatalytic activity depends on the nature of the reactants and on the overall process at the catalyst surface resulting from competition of various elementary phenomena. TiO_2 nanoparticles are crystallized into two main polymorphic forms: anatase and rutile. Anatase TiO_2 nanoparticles are more active as a photocatalyst than rutile nanoparticles [1]. The third crystal phase, and a less common form of titanium dioxide, is brookite. The rutile phase is the stable phase at high temperature, but anatase and brookite are common in fine-grained natural and synthetic samples [2].

In 1972, Formenti et al. [3] synthesized several metal oxide particles with diameters in the range from 10 to 200 nm by carrying the vapor of metal chloride in a hydrogen–oxygen flame. Yang et al. [4] used three different burners to obtain a wide range of flame processing conditions. Mixtures of anatase and rutile-phased titania nanoparticles were obtained at low reaction temperatures between 900 and 1430 °C. Spherical particles of 100% anatase titania were obtained at high temperatures between 1500 and 1570 °C. Yeh et al. [5] also reported that the anatase fraction of titania particles created in flames increased with an increase of oxygen concentration in the oxidizer.

Anatase TiO_2 nanoparticles can be transformed to rutile when heated. It is well known that the onset temperature of the phase transition is influenced by cation impurities, anion impurities, grain size, reaction atmosphere, synthesis condition, and other factors [6]. The onset temperatures for the transformation of prepared anatase particles into rutile particles using heat treatment range from 650 to 800 °C depending on the compact structure of the pellet [7] and the contents of the silica additive [6]. Xia et al. [8] also showed the same transformation of anatase particles into rutile particles by heat treatment of titania nanoparticles prepared by vapor-phase hydrolysis.

* *Corresponding author*. Tel.: +82 63 270 3997; fax: +82 63 270 2460.
E-mail address: gwlee@chonbuk.ac.kr (G.W. Lee).

1044-5803/$ – see front matter © 2009 Elsevier Inc. All rights reserved.
doi:10.1016/j.matchar.2009.08.001

Table 1 – Experimental conditions and tube inner diameters of burner.

Gas	Ar	H_2	O_2	Air	TTIP evaporation temperature	Ultrasonic processor (VCX-750)
Function	TTIP carrier gas	Fuel	Oxidizer		80 °C	To reduce particle size
Flow rates (liters per minute)	0.3	2.0	3.7	30.0		0, 20, 60% of its max. amplitude
Tube inner diameter (mm)	3.9	16.6	70.0			

In 2000, Zhang and Banfield [9] studied the kinetics of phase transformation of nanocrystalline anatase samples using X-ray diffraction at temperatures ranging from 600 to 1150 °C. They reported that the activation energy of nucleation of rutile particles were size-dependent. Also, the effects of aging on the crystalline phases, crystalline sizes, and sintering properties of TiO_2 gels were investigated by Hsiang and Lin [10]. They showed that the hydroxyl ions existing in the anatase lattice decreased with increasing aging time, and so the oxygen vacancy concentration produced after calcination decreased.

The particle size effect on the phase transformation of nanocrystalline TiO_2 was reported in [11]. The TiO_2 powders were obtained by the solvothermal method. Kim et al. [11] reported that the smaller-sized powders tended to be transformed to rutile more easily than the larger-sized powders. Zhu et al. [12] also reported the size effect on the phase transformation sequence of heat-treated TiO_2 nanocrystals prepared by the sol-gel method. The effects of grain size and phase content on the transition were studied for TiO_2 nanocrystals annealed in air for 1 h for a temperature range of 200 to 650 °C. Their results indicated that the phase transition sequence depends on the relative grain size between anatase and brookite.

We investigated the effect of ultrasonic processing on the phase transition of TiO_2 nanoparticles from anatase to rutile when heated. The TiO_2 nanoparticles were synthesized using a coflow hydrogen diffusion flame. An ultrasonic processor was used to change the diameters of the formed TiO_2 nanoparticles to those having a similar anatase fraction.

2. Experimental

The experimental setup consisted of several gases and mass flow controllers with readout units (Kofloc Co. Ltd.), a burner and a flame used as a hydrolysis reactor, a horizontal traverse with a controller for particle sampling, and a two-dimensional traverse system for moving the burner and the precursor evaporator. The burner used in this study consisted of three concentric tubes of 3.87, 16.57, and 70.0 mm inner diameters. The argon gas used as a carrier gas for the precursor was delivered through the central tube via the evaporator of the TTIP precursor ($Ti[OCH(CH_3)_2]_4$, titanium tetraisopropoxide,

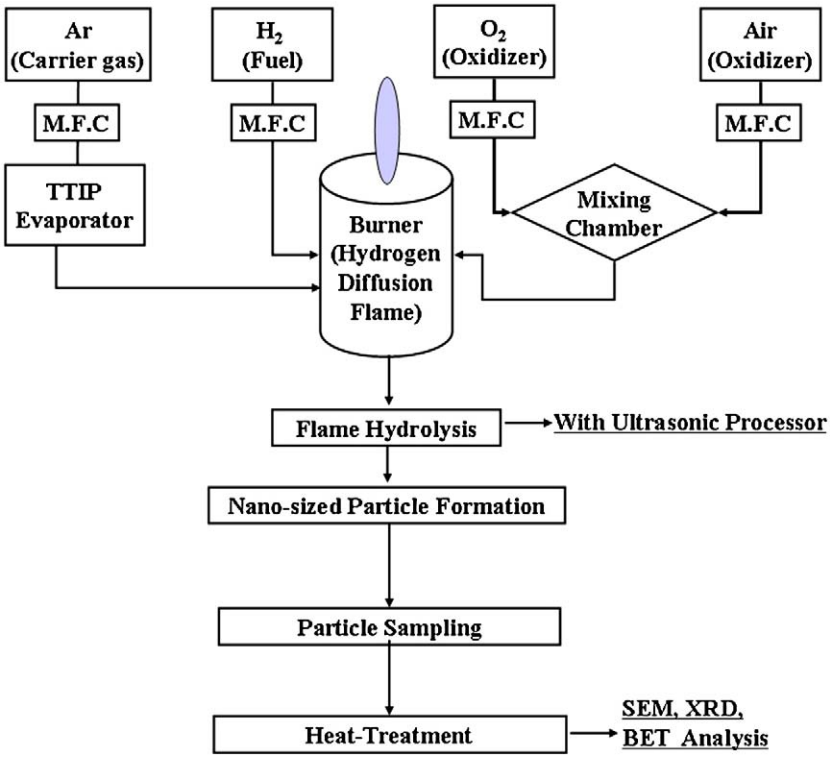

Fig. 1 – Schematic diagrams of experimental procedure.

Kanto Chemical Co., Inc., purity >97%). The precursor was used without additional purification. The evaporator was maintained at a temperature of 80 °C. The fuel was hydrogen, supplied through the second tube. The oxygen was premixed with air, and then the mixture was passed through the outer (third) tube. The experimental conditions regarding the flowrates of the gases are provided in Table 1.

To reduce the size of the formed TiO_2 nanoparticles, an ultrasonic processor (VCX-750, Sonic & Materials Inc.) was used. The net power output of the ultrasonic processor was 750 W. A sonication probe having a 13 mm tip diameter was placed 65 mm away from the center of the flame in the radial direction. Also, the tip of the probe was located at a height of 31 mm above the burner in the axial direction. The amplitude of the ultrasonic processor was varied from 0 to 60% of its maximum capacity to change the diameters of the formed TiO_2 nanoparticles.

The synthesized nanoparticles were sampled on thermophoretic plates placed at 230 mm height above the burner (HAB). The crystalline phases of the collected TiO_2 nanoparticles from the plates were analyzed using X-ray diffraction (XRD) (Rigaku Inc., DMAX-2500), and the particle characteristics were analyzed using FE-SEM (Hitachi Inc., S-4700) and BET (Micrometritics Co., Tristar 3000). Based on the preliminary XRD analysis, the flowrates of several gases for the flame synthesis of the anatase-phased TiO_2 nanoparticles were

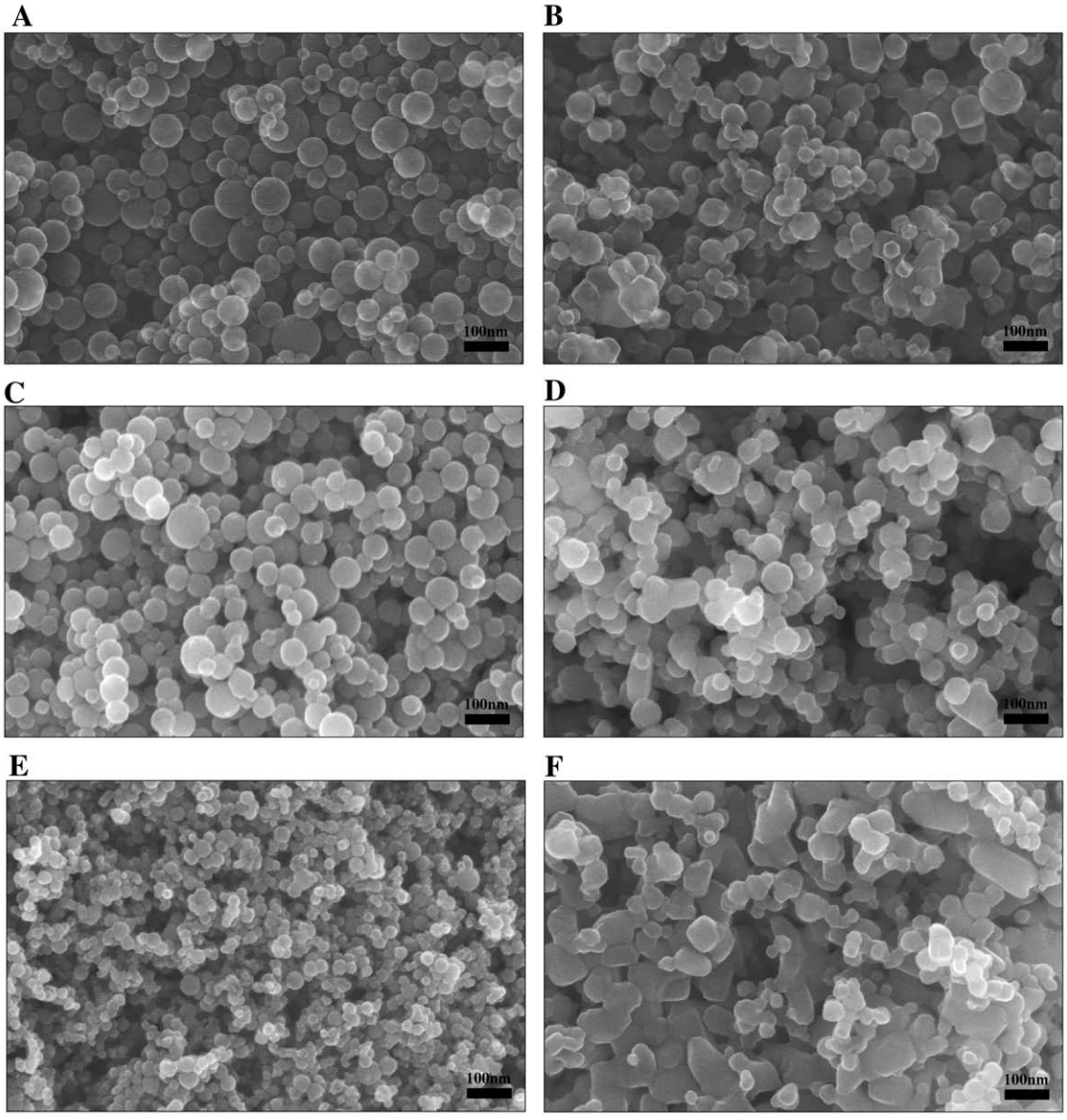

Fig. 2 – SEM images of heat-treated flame-synthesized TiO_2 nanoparticles formed without/with using ultrasonic processor, (A) without using ultrasonic processor, heat-treated at 200 °C for 30 min, (B) without using ultrasonic processor, heat-treated at 800 °C for 30 min, (C) with using 20% amplitude of ultrasonic processor, heat-treated at 200 °C for 1 h, (D) with using 20% amplitude of ultrasonic processor, heat-treated at 800 °C for 1 h, (E) with using 60% amplitude of ultrasonic processor, heat-treated at 200 °C for 1 h, (F) with using 60% amplitude of ultrasonic processor, heat-treated at 800 °C for 1 h.

selected. The formed nanoparticles were collected on the thermophoretic plate. To investigate their thermal stability, the collected anatase nanoparticles were heat treated at 200, 700, and 800 °C. A schematic diagram of the experimental procedure is shown in Fig. 1.

3. Results and Discussion

The oxygen content in the oxidizer mixture was about 29.7 vol.%, as given in Table 1. The measured maximum centerline temperature was 1743 °C at 60 mm HAB [13]. In our previous study [13], most of the formed nanoparticles were of the anatase-phase with diameters ranging from 30 to 60 nm for the same experimental conditions. For the case of not using the ultrasonic processor, the data from our previous work [13] were used as shown in the SEM images (Fig. 2(A) and (B)) and the XRD patterns (Fig. 3).

Fig. 2(A) and (B) shows SEM images of the synthesized TiO_2 nanoparticles without using the ultrasonic processor after heat-treatment at 200 and 800 °C, respectively, for 30 min. The heat-treatment temperature of 200 °C was selected for drying the formed nanoparticles. Another temperature, 800 °C, was selected for the sintering and phase transformation of the anatase TiO_2 nanoparticles. Fig. 2(A) shows that most of the formed nanoparticles have diameters ranging from 30 to 60 nm. After the heat treatment at 800 °C (Fig. 2(B)), the sizes and shapes of the nanoparticles had not changed significantly.

Fig. 2(C) to (F) also show SEM images of the synthesized TiO_2 nanoparticles using the ultrasonic processor at 20 and 60% of its maximum amplitude. In Fig. 2(C), the formed nanoparticles are almost the same sizes and shapes as those shown in Fig. 2(A). After heat treatment at 800 °C (Fig. 2(D)), although some agglomerates are seen, there are no significant changes in the sizes and shapes of the nanoparticles. However, as Fig. 2(E) shows, formed nanoparticles have diameters ranging from approximately 20 to 30 nm using 60% of the maximum ultrasonic amplitude. This size range is much smaller than that of the particles shown in Fig. 2(A) and (C) for 0 and 20% of maximum ultrasonic amplitude, respectively. After heat treatment at 800 °C (Fig. 2(F)), most of the particles were sintered and showed much larger clusters.

To obtain quantitative data for the variation in particle size distributions, BET surface areas of the nanoparticles were measured. When the ultrasonic processor was used at 20% of its maximum sonication amplitude, the specific surface areas were 32.7, 27.4, and 21.5 m^2/g for the heat treatments at 200, 700, and 800 °C, respectively. Due to the sintering of the particles at the heat treatment temperature of 800 °C, the specific surface area decreased from 32.7 to 21.5 m^2/g. For the case of using the ultrasonic processor at 60% of its maximum amplitude, the specific surface area of the formed nanoparticles was 69.1 m^2/g. Compared with the value of 32.7 m^2/g for the case of 20% amplitude, this result means that much smaller nanoparticles were synthesized. Due to the sintering among the particles, the surface areas were reduced to 30.7 and 12.3 m^2/g as the heat treatment temperatures increased to 700 and 800 °C, respectively.

On the basis of the SEM images in Fig. 2 and BET surface area analysis, the smaller nanoparticles were sintered more easily than the larger nanoparticles. Also, it is possible to produce much smaller nanoparticles at the same flame-synthesis condition using the ultrasonic processor.

To verify this observation, XRD patterns are shown in Figs. 3 and 4. Fig. 3(A) shows the XRD patterns of nanoparticles formed without using the ultrasonic processor after heat treatment at 200, 700, and 800 °C for 30 min. Only the case of 800 °C shows a small increment in rutile content at $2\theta = 27.5°$ for the (110)

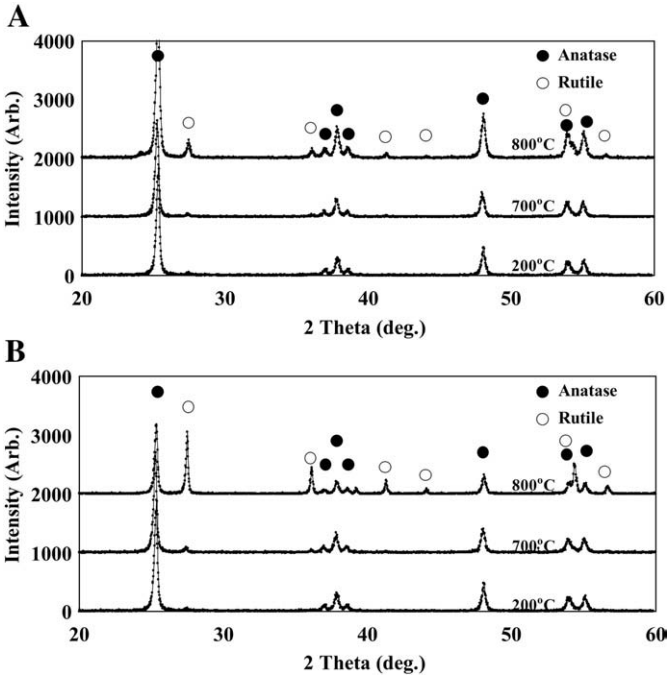

Fig. 3 – XRD patterns of flame-synthesized TiO_2 nanoparticles without using ultrasonic processor, heat-treated at 200, 700, and 800 °C for (A) 30 min, and (B) 3 h.

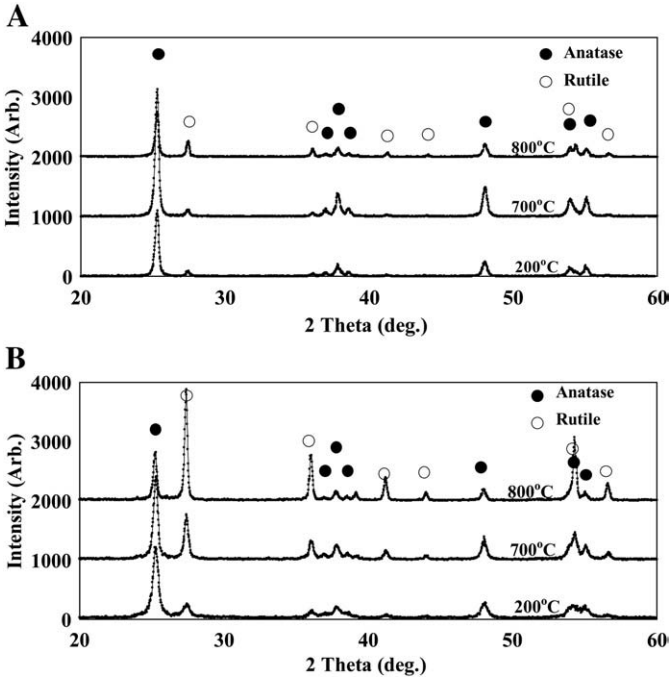

Fig. 4 – XRD patterns of flame-synthesized TiO_2 nanoparticles heat-treated at 200, 700, and 800 °C for 1 h, with using ultrasonic processor at (A) 20%, and (B) 60% of its maximum amplitude.

reflection. For a heat treatment duration of 3 h, the rutile content of the nanoparticles increased as shown in Fig. 3(B). Similarly, at 20% of the maximum amplitude of the ultrasonic processor, Fig. 4(A) shows the XRD patterns of the nanoparticles after heat treatment at 200, 700, and 800 °C for 1 h. Similar to the results shown in Fig. 3(A), Fig. 4(A) shows a small increment in rutile content for the case of 800 °C heat treatment. However, for 60% of the maximum amplitude of the ultrasonic processor, Fig. 4(B) shows a much higher fraction of rutile phases for 700 and 800 °C heat treatment for 1 h than the results shown in Figs. 3(A) and 4(A).

Based on XRD analysis, the flame-generated TiO_2 nanoparticles synthesized using the ultrasonic processor at 60% of its maximum amplitude appeared to be transformed from anatase to rutile phase more easily than those formed with or without the ultrasonic processor at 20% of its maximum amplitude. The change in anatase content for the three heat treatment temperatures is plotted in Fig. 5. The weight fractions of anatase were calculated from the measured XRD intensities of the strongest peaks, showing anatase ($2\theta = 25.3°$ for the (101) reflection) and rutile ($2\theta = 27.5°$ for the (110) reflection) using a formula developed by Spurr and Myers [14]. The anatase content of nanoparticles heat treated at 200 °C for 0, 20, and 60% of the maximum amplitude of the ultrasonic processor are 96.2, 90.4, and 81.8 wt.%, respectively. Anatase fractions of formed nanoparticles were reduced by only 15% using the ultrasonic processor at 60% of its maximum amplitude compared to not using the processor. Based on the specific surface areas and XRD patterns, the decreased size of synthesized particles could be the reason for

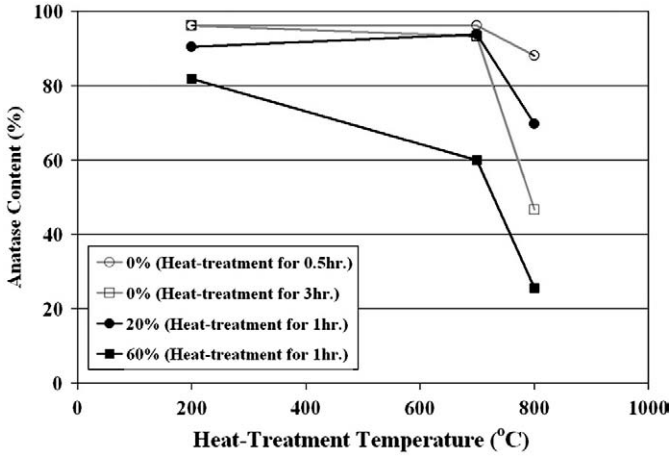

Fig. 5 – Weight fractions of anatase-phased TiO_2 nanoparticles with several heat treatment temperatures.

Table 2 – Measured specific surface areas and calculated particle diameters.

Sonication amplitude (of max.)		20%		60%	
		Specific surface area (m^2/g)	Calculated diameter (nm)	Specific surface area (m^2/g)	Calculated diameter (nm)
Heat-treatment (°C)	200	32.7	49.7	69.1	21.9
	700	27.4	55.8	30.7	48.3
	800	21.5	69.7	12.3	116.6

the reduced anatase content of the particles. The smaller particles formed in the flame could be transformed to rutile more easily when synthesized through the flame. For heat treatment at 800 °C when the ultrasonic processor was not used, the anatase fractions are 88.1 and 46.6 wt.% for heat treatment times of 30 min and 3 h, respectively. Using 20 and 60% of the maximum amplitude of the ultrasonic processor, the anatase content is 69.7 and 25.6 wt.%, respectively.

On the basis of specific surface areas, the anatase phase fractions, and particle densities, particle diameters were calculated and are shown in Table 2. Due to the use of the ultrasonic processor, the particle diameters decreased from 49.7 to 21.9 nm. Thus, for the case of 60% amplitude, the ultrasonic waves may prevent the primary particles from growing or sintering to larger particles. For heat treatment at 800 °C, the particles were sintered and the diameters increased from 21.9 to 116.6 nm at 60% amplitude.

As shown by the SEM images, particle diameters, and XRD patterns, the smaller anatase TiO_2 nanoparticles flame-synthesized with the ultrasonic processor were more easily transformed to rutile. Also, reducing the sizes of the flame-synthesized nanoparticles using the ultrasonic processor without inducing significant changes in their crystalline phases is possible.

4. Conclusion

The effect of ultrasonic processing on the phase transformation of flame-synthesized anatase TiO_2 nanoparticles to rutile was investigated. TiO_2 nanoparticles with varied size ranges were prepared using a coflow hydrogen diffusion flame and an ultrasonic processor. Smaller nanoparticles having similar anatase phase content using the ultrasonic processor were produced. Based on SEM images and BET surface areas, the smaller nanoparticles were sintered more easily than larger nanoparticles. From XRD analysis, we showed that when heated, the TiO_2 nanoparticles synthesized using the ultrasonic processor at 60% of its maximum amplitude transformed from the anatase phase to the rutile phase more easily than those formed with or without the ultrasonic processor operated at 20% of its maximum amplitude.

Acknowledgement

This work was supported by the Automobile Hi-Technology Research Center, Engineering Research Institute of CNU (Chonbuk National University).

REFERENCES

[1] Znaidi L, Seraphimova R, Bocquet JF, Colbeau-Justin C, Pommier C. A semi-continuous process for the synthesis of nanosize TiO_2 powders and their use as photocatalysts. Mater Res Bull 2001;36:811–25.
[2] Chen X, Mao SS. Titanium dioxide nanomaterials: synthesis, properties, modifications, and applications. Chem Rev 2007;107:2891–959.
[3] Formenti M, Juillet F, Meriaudeau P, Teichner SJ, Vergnon P. Preparation in a hydrogen–oxygen flame of ultrafine metal oxide particles. Oxidative properties toward hydrocarbons in the presence of ultraviolet radiation. J Colloid Interface Sci 1972;39:79–89.
[4] Yang G, Zhuang H, Biswas P. Characterization and sinterability of nanophase titania particles processed in flame reactors. Nanostruct Mater 1996;7:675–89.
[5] Yeh CL, Yeh SH, Ma HK. Flame synthesis of titania particles from titanium tetraisopropoxide in premixed flames. Powder Technol 2004;145:1–9.
[6] Okada K, Yamamoto N, Kameshima Y, Yasumori A, MacKenzie KJD. Effect of silica additive on the anatase-to-rutile phase transition. J Am Ceram Soc 2001;84:1591–6.
[7] Park J-K, Ahn J-P, Kim G. Effect of compact structure on phase transformation kinetics from anatase phase to rutile phase and microstructure evolution during sintering of ultrafine titania powder compacts. Met Mater Int 1999;5:129–35.
[8] Xia B, Huang H, Xie Y. Heat treatment on TiO_2 nanoparticles prepared by vapor-phase hydrolysis. Mater Sci Eng B 1999;57:150–4.
[9] Zhang H, Banfield JF. Phase transformation of nanocrystalline anatase-to-rutile via combined interface and surface nucleation. J Mater Res 2000;15:437–48.
[10] Hsiang HI, Lin SC. Effects of aging on the phase transformation and sintering properties of TiO_2 gels. Mater Sci Eng A 2004;380:67–72.
[11] Kim C-S, Kwon I-M, Moon BK, Jeong JH, Choi B-C, Kim JH, et al. Synthesis and particle size effect on the phase transformation of nanocrystalline TiO_2. Mater Sci Eng C 2007;27:1343–6.
[12] Zhu K-R, Zhang M-S, Hong J-M, Yin Z. Size effect on phase transition sequence of TiO_2 nanocrystal. Mater Sci Eng A 2005;403:87–93.
[13] Lee GW, Choi SM. Thermal stability of heat-treated flame-synthesized anatase TiO_2 nanoparticles. J Mater Sci 2008;43:715–20.
[14] Spurr RA, Myers H. Quantitative analysis of anatase–rutile mixtures with an X-Ray diffractometer. Anal Chem 1957;29:760–2.